# SUPPORTING INFORMATION

# Cautionary tale of using tris(alkyl)phosphine reducing agents with $NAD^+$-dependent enzymes

*Sagar M. Patel[†], Thomas G. Smith[‡], Martha Morton[‡], Kyle M. Stiers[§], Javier Seravalli[†], Stephen J. Mayclin[¥], Thomas E. Edwards[¥], John J. Tanner[§], and Donald F. Becker[*,†]*

[†]Department of Biochemistry and Redox Biology Center, and [‡]Chemistry, University of Nebraska-Lincoln, Lincoln, Nebraska 68588, United States. [§]Department of Biochemistry, University of Missouri, Columbia, Missouri 65211, United States. [¥]UCB Pharma, Seattle Structural Genomics Center for Infectious Disease, Bainbridge Island, WA 98110, United States.

**Corresponding Author**
Donald F. Becker
Department of Biochemistry and Redox Biology Center, University of Nebraska-Lincoln, Lincoln, Nebraska 68588, United States;
*Email: dbecker3@unl.edu

## TABLE OF CONTENTS

## EXPERIMENTAL PROCEDURES

### Materials and Reagents

MilliQ-Ultra purified water was used for the preparation of all buffers and chemicals in the experiments. The following reagents were purchased from Millipore-Sigma: $NaH_2PO_4$, ε-Amino-N-Caproic Acid, N-tosyl-L-phenylalanine chloromethyl ketone, bovine serum albumin, pyruvate, L-lactate dehydrogenase, NADPH, NADH, and $NH_4F$. The following reagents were commercially available from Fisher Scientific: NaOH, NaCl, 2-[4(2-hydroxyethyl)piperazin-1-yl]ethanesulfonic acid (HEPES), $Na_2CO_3$, $NaHCO_3$, and ethylenediamine tetraacetic acid (EDTA) disodium salt. Reagents β-octyl-D-glucopyranoside (β-OG) and L-proline were commercially available from Combi-Blocks. Ethanol (190- or 200-proof) was purchased from Decon Labs. Tris(hydroxymethyl)aminomethane (Tris), glycine, isopropyl β-D-thiogalactopyranoside (IPTG), phenylmethylsulfonyl fluoride (PMSF), leupeptin hemisulfate, and $NAD^+$ were purchased from Gold Biotechnology. Imidazole and *o*-aminobenzaldehyde (*o*-AB) were purchased from Acros Organics. In terms of tris(alkyl) phosphine reducing agents used in this study, Tris(3-hydroxypropyl)phosphine (THPP) was purchased from Strem Chemicals, and the hydrochloride salt of Tris(2-carboxyethyl)phosphine (TCEP-HCl) was purchased from ThermoFisher Scientific-Pierce Biotech.

Stock solutions of NADH and $NAD^+$ were prepared in 10 mM Tris-HCl (pH 8) and stored at -80 °C. NADH and $NAD^+$ concentrations were determined spectrophotometrically at wavelengths 340 nm ($\varepsilon_{340}$ = 6220 $M^{-1}cm^{-1}$)[1] and 260 nm ($\varepsilon_{260}$ = 17,370 $M^{-1}cm^{-1}$),[2] respectively. Stock solutions of each tris(alkyl)phosphine reducing agent, THPP and TCEP, were made at pH 7.5 in 0.1 M Tris-HCl (pH 7.5) buffer and stored at -80 °C.

### PYCR and reversible activity assays

Human PYCR1 (UniProt ID P32322) was expressed and purified as described previously.[3] Similarly, PYCR2 (UniProt ID Q96C36) was expressed from a pKA8H-PYCR2 construct in *E. coli* BL21 (DE3) pLysS competent cells (Novagen-EMD Millipore Sigma), cultured in TB liquid media and induced with 0.4 mM IPTG. After centrifugation, cell pellets were resuspended in NPI-5 cell lysis buffer (5 mM imidazole, 500 mM NaCl, 50 mM $NaH_2PO_4$, pH 7.5) supplemented with 500 µM THPP, 0.01% TritonX-100 detergent (Amresco), 0.01% Brij-35 polyoxyethylene detergent (Santa-Cruz Biotechnology), 10 mM β-OG, and a mixture of five protease inhibitors. The cell suspension was then subjected to sonication to lyse the cells followed by centrifugation at 4 °C. The supernatant was then applied to a Ni-NTA Superflow (Qiagen) affinity column for purification PYCR2.

The ability of human PYCR1 and PYCR2 to catalyze the reverse reaction (L-proline + $NAD^+$ → L-P5C + NADH) was tested in 0.1 M Tris-HCl (pH 7.5) buffer containing 0.01% (v/v) Brij-35 detergent, 30 mM $MgCl_2$, 5 mM L-proline, and 0.5 mM $NAD^+$, and with or without tris(alkyl)phosphine compound (1 mM TCEP (pH 7.5) or 1 mM THPP (pH 7.5)). Assays (600 µl total volume) were performed at room temperature and initiated by adding PYCR enzyme (0.06 µM final concentration). Reaction components were kept covered with aluminum foil to protect from ambient light and the assays were performed

in the dark. Reactions were monitored at 340 nm for 30 min in a 1-cm path length quartz cuvette (Starna Cells) using a Varian Cary 50-UV/VIS spectrophotometer (Agilent Technologies).

**Glucose-6-phosphate dehydrogenase (G6PDH) assays**

G6PDH from *Leuconostoc mesenteroides* was purchased from Millipore-Sigma (catalog number G5760-1KU). Assays were performed in an Epoch 2 plate reader (BioTek, Winooski, VT, USA) by monitoring NADH at 340 nm. Each assay contained G6PDH (2000x dilution), 5 mM G6P, and variable amounts of $NAD^+$ and TCEP in 50 mM MOPS (pH 7.4) buffer.

**$NAD^+$ reactions with tris(alkyl)phosphine reagents**

Reactions of $NAD^+$ with THPP and TECP were initially performed at room temperature under dark conditions similarly to the PYCR enzyme assays above except that no enzyme was added. Reaction components (0.5 mM $NAD^+$ and 5 mM L-proline) were incubated in 0.1 M Tris-HCl buffer (pH 7.5, 0.01% (v/v) Brij-35 detergent, 30 mM $MgCl_2$) for 15 min in a quartz cuvette followed by the addition of THPP and TCEP (1 mM final concentration). The absorbance at 340 nm was monitored for a total of 30 min using a Varian Cary 50-UV/VIS spectrophotometer.

Stopped-flow kinetics of the reaction between $NAD^+$ and THPP and TCEP were performed in the dark with different reaction buffers of 100 mM (pH 7.5) HEPES, Tris-HCl, Na-phosphate, and PBS. All stopped-flow experiments were conducted on a Hi-Tech Scientific SF-61DX2 stopped-flow instrument equipped with a photodiode array detector and KinetAsyst software. The temperature of the mixing chamber for all experiments was maintained at room temperature (23 $^oC$). $NAD^+$ (0.5 mM final concentration) was rapidly mixed with THPP or TCEP (25 mM final concentration) and the reaction was monitored in the stopped-flow instrument by multiwavelength absorption in the range of 300-700 nm. In another set of experiments, $NAD^+$ was held fixed at 0.5 mM (after mixing) while increasing the concentrations of THPP and TCEP (5-150 mM after mixing) in 100 mM HEPES (pH 7.5) buffer and monitoring the reaction by single wavelength data collection at 334 nm. The average of three collected traces (n=3 technical replicates) was fit by non-linear least-squares regression to a single 3-parameter exponential rise equation using SigmaPlot 12.0 (version 12.0.0.182, Systat Software). The observed rate constant ($k_{obs}$) from the single exponential fitting was then plotted versus THPP and TCEP concentrations from which the apparent second order rate constant for the forward step of the reaction ($k_+^{app}$) was determined by linear least squares fit analysis. The apparent first-order rate constant for the reverse step of the reaction ($k_-^{app}$) was determined by the intercept at the vertical axis. Under the pseudo-first-order conditions of the stopped-flow experiments ([THPP or TCEP] >> [$NAD^+$]):

$$k_{obs} = (k_+^{app})\,[\text{THPP or TCEP}] + (k_-^{app})$$

and the apparent association equilibrium constant is defined as $K_a^{app} = (k_+^{app}/k_-^{app})$.[4]

**Nuclear Magnetic Resonance (NMR) characterization of the reaction product**

For NMR measurements, the reaction of $NAD^+$ with THPP and TCEP was performed in 100 mM $NaHCO_3$-$Na_2CO_3$ (pH 7.5) buffer. The reaction was protected from ambient light by performing all steps in the dark and covering the samples with aluminum foil. Samples were made by reacting $NAD^+$ (30.6 mM) or NADH (25.3 mM) with THPP or TCEP (400 mM) and kept on ice prior to NMR measurements. We prepared each reaction component individually as well as in approximate (1:1) volume combinations of $NAD^+$ to THPP and TCEP. The total sample volume was 500 µL, including 50 µL deuterium oxide that was added for spectrometer lock. NMR experiments that were performed include: one-dimensional $^1H$, $^{13}C$, and $^{31}P$, as well as two-dimensional $^1H$-$^1H$ COSY, $^1H$-$^1H$ TOCSY, $^1H$-$^{31}P$ HSQC-TOCSY, $^1H$-$^{31}P$ HSQC, $^1H$-$^{13}C$ HMBC, and $^1H$-$^{13}C$ HSQC. The NMR spectra were acquired on a Bruker Avance 600 MHz NMR spectrometer with a 5 mm TXI or 5 mm BBO probe, held at 4 $^oC$. All spectra were acquired under dark lab conditions with overhead lights off the entire time.

**Crystal structure determination of short-chain dehydrogenase/reductase (SDR)**

The gene *BamMC406_2208* (UniProt ID B1YU47) from *Burkholderia ambifaria* strain MC40-6 encodes a 259 amino acid long open reading frame (ORF) annotated as a short chain dehydrogenase/reductase SDR. The gene was cloned from genomic DNA into the BG1861 expression vector which encodes an N-terminal hexahistidine affinity tag; the full polypeptide sequence is MAHHHHHH-(ORF). The protein was expressed and purified using a general expression and purification protocol detailed previously.[5, 6] The protein was expressed in BL21 (DE3) R3 Rosetta *E. coli* cells. The protein was purified by nickel immobilized metal affinity chromatography (Ni-IMAC) followed by size exclusion chromatography (SEC) in 20 mM HEPES pH 7.0, 300 mM NaCl, 1 mM TCEP, and 5% v/v glycerol, concentrated to 16.34 mg/ml, and stored at -80 °C prior to crystallization experiments. The SSGCID target identifier is BuamA.00010.o and the SSGCID construct identifier is BuamA.00010.o.B1 with a protein batch number of PS38204. The plasmid and the protein are available (**www.ssgcid.org/available-materials/**). Crystals of BuamA.00010.a.B1 were grown at 20.8 mg/mL with 5 mM NADP using the sitting drop vapor diffusion method at 14 °C. Equal volumes of the protein and precipitant were equilibrated against 80 µL of reservoir in Compact Jr 96-well crystallization plates from Rigaku Reagents. The crystals were obtained from the MCSG1 crystallization screen (Microlytic, now Anatrace) in 100 mM potassium tartrate with 25% PEG 3350. The crystals were harvested into reservoir supplemented with 8 mM NADP and 20% ethylene glycol as cryo-protectant then flash frozen in liquid nitrogen. A data set was obtained at the Advanced Light Source beamline 8.2.1 equipped with an ADSC quantum 315r CCD detector at a wavelength of 1.00 Å under a stream of nitrogen (100K). Data were reduced with XDS/XSCALE.[7] The structure was determined by molecular replacement in Molrep[8] using PDB ID 5IDX (SSGCID, no primary citation) as a search model. The final model was obtained after numerous iterative rounds of refinement in Phenix[9] and manual model building in Coot.[10] The coordinates and structure factor files have been deposited to the Protein Data Bank with PDB ID 5VPS. X-ray diffraction images are available at the Integrated Resource for Reproducibility in Macromolecular Crystallography **(www.proteindiffraction.org).**

**SI Table 1. Pre-steady-state kinetic parameters for the reaction of $NAD^+$ and tris(alkyl)phosphine compounds**

| Kinetic parameter | THPP | TCEP |
|---|---|---|
| $k_+^{app}$ ($M^{-1}$ $s^{-1}$)[a] | 231 ± 6 | 491 ± 25 |
| $k_-^{app}$ ($s^{-1}$)[b] | 6.6 ± 0.4 | 24 ± 2 |
| $K_a^{app}$ ($M^{-1}$)[c] | 35 ± 2 | 20 ± 2 |

[a]Value ± Std error is reported for the apparent forward rate constant determined as the slope of the plotted data fit to a linear least-squares equation using SigmaPlot 12.0 (version 12.0.0.182, Systat Software) with data plotted as (mean ± SD) of n=3 technical replicates
[b]Value ± Std error is reported for the apparent reverse rate constant determined as the vertical axis intercept of the plotted data
[c]Apparent equilibrium association constant determined from the calculation of $K_a^{app} = (k_+^{app}/k_-^{app})$

**SI Table 2. NMR data from $^1H$-$^{13}C$ correlation experiments† of $NAD^+$**

| Label | δ ($^1H$, ppm)‡ | δ ($^{13}C$, ppm) | HMBC |
|---|---|---|---|
| **2** | 9.1 (s, 1H) | 138.0 | 3, 4, 6, 7, 8 |
| **3** | | 131.6 | |
| **4** | 8.57 (d, 1H, 8.5 Hz) | 143.6 | 2, 6, 7 |
| **5** | 7.93 (at, 1H, 6.6 Hz) | 126.6 | 3, 6 |
| **6** | 8.9 (d, 1H, 6.6 Hz) | 140.3 | 2, 4, 5, 8 |
| **7** | | 163.2 | |
| **8** | 5.85 (d, 1H, 5.6 Hz) | 98 | 2, 6 |

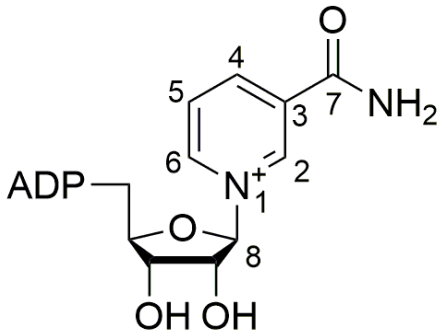


†Chemical shifts were determined from the one dimensional $^1H$ and $^{13}C$ experiments. Correlations were determined from $^1H$-$^{13}C$ HSQC and HMBC experiments and correspond to site labels shown above in $NAD^+$ structure.
‡Listed next to each $^1H$-NMR chemical shift value is (multiplicity designation [s, singlet; d, doublet; etc.], integral value, and J-coupling constant).

**SI Table 3. NMR data from $^{1}$H-$^{13}$C correlation experiments† of NADH**

| Label | δ ($^{1}$H, ppm)‡ | δ ($^{13}$C, ppm) | HMBC |
|---|---|---|---|
| **2'** | 6.68 (s, 1H) | 136.7 | 3', 4', 6', 7', 8' |
| **3'** | | 97.5 | |
| **4'** | 2.35 (dd, 1H, 3.4 and 18.8 Hz), 2.49 (d, 1H, 18.4 Hz) | 19.9 | 2', 3', 5', 6' |
| **5'** | 4.51 (1H) | 103.4 | 3', 6' |
| **6'** | 5.73 (d, 1H, 8.4 Hz) | 121.4 | 2', 4', 5', 8' |
| **7'** | | 170.7 | |
| **8'** | 4.55 (d, 1H, 7.1 Hz) | 93.1 | 2', 6' |

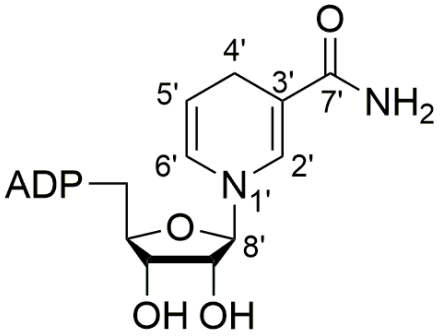


†Chemical shifts were determined from the one dimensional $^{1}$H and $^{13}$C experiments. Correlations were determined from the HMBC experiment and correspond to site labels shown above in NADH structure.

‡Listed next to each $^{1}$H-NMR chemical shift value is (multiplicity designation [s, singlet; d, doublet; dd, doublet of doublets], integral value, and J-coupling constant).

**SI Table 4. NMR data from $^{1}H$-$^{31}P$ correlation experiments† of $NAD^{+}$ and THPP reaction mixture**

| Label | δ ($^{1}H$, ppm)‡ | δ ($^{1}H$-$^{31}P$ HSQC, ppm) | δ ( $^{1}H$-$^{31}P$ HSQC-TOCSY, ppm) |
|---|---|---|---|
| **2** | 9.11 (s) | | 34.3 |
| **2''** | 7.10 (d, 1H, 1.8 Hz), minor 7.23 (d, 1H, J = 1.8 Hz) | 34.3, minor 34.4 | 34.3, minor 34.4 |
| **4** | 8.59 (d, J = 8.4 Hz) | | 34.3 |
| **4''** | 3.96 (1H), minor 4.35 | 34.3, minor 34.4 | 34.3, minor 34.4 |
| **6** | 8.91 (d, J = 6.3 Hz) | | 34.3 |
| **6''** | 6.33 (at, 1H, J = 6.3 Hz), minor 6.28 (at, 1H J = 6.3) | 34.3, minor 34.4 | 34.3, minor 34.4 |
| **9''** | 1.96 (m), minor 1.98 | 34.3 | 34.3 |
| **10''** | 1.54 (m) | 34.3 | 34.3 |
| **11''** | 3.44 (m) | | 34.3 |

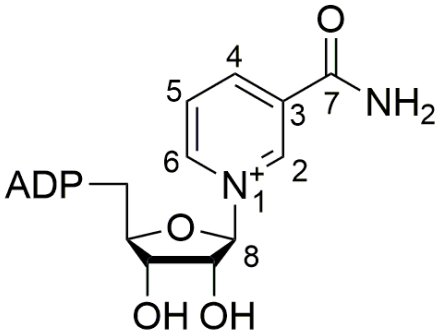


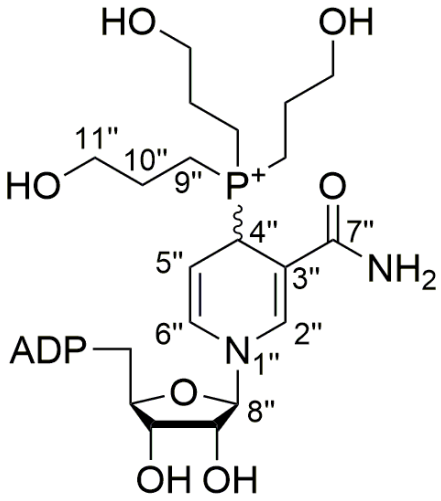


†Chemical shifts were determined from the one dimensional $^{1}H$ and $^{31}P$ experiments. Correlations were determined from $^{1}H$-$^{31}P$ HSQC and HSQC-TOCSY experiments shown in Fig. 2 and SI Fig. 5, respectively and correspond to site labels shown above in the $NAD^{+}$ structure and $NAD^{+}$—THPP reaction product structure.

‡Listed next to each $^{1}H$-NMR chemical shift value is (multiplicity designation [s, singlet; d, doublet; m, multiplet; etc.], integral value, and J-coupling constant).

Note the $^{1}H$-$^{31}P$ HSQC-TOCSY correlations listed here correspond to both $NAD^{+}$—THPP reaction product protons and to $NAD^{+}$ protons.

**SI Table 5. NMR data from $^{1}H$-$^{13}C$ correlation experiments† of $NAD^{+}$ and THPP reaction mixture**

| Label | δ ($^{1}H$, ppm)‡ | δ ($^{13}C$, ppm)‡ | HMBC |
|---|---|---|---|
| **2''** | 7.10 (d, 1H, 1.8 Hz), minor 7.23 (d, 1H, 1.8 Hz) | 139.3, minor 134.5 | 3'', 4'', 6'', 7'', 8'' |
| **3''** | | 94.6 | |
| **4''** | 3.96 (1H), minor 4.35 | 28.4 (47 Hz), minor 28.6 (48 Hz) | 2'', 3'', 5'', 6'', 7'' |
| **5''** | 4.51 | 93.9 | 4'', 6'' |
| **6''** | 6.33 (at, 1H, 6.3 Hz), minor 6.28 (at, 1H, 6.3 Hz) | 126.6, minor 132.6 | 2'', 4'', 5'', 8'' |
| **7''** | | 168.2 | |
| **8''** | 4.67 (broad s), minor 4.69 | 92.6, minor 92.3 | 2'', 6'' |
| **9''** | 1.96 (m), minor 1.98 | 11.3 (44 Hz), minor 11.1 (45 Hz) | 10'', 11'' |
| **10''** | 1.54 (m) | 21.6 (4 Hz), minor 21.8 (4 Hz) | 9'', 11'' |
| **11''** | 3.44 (m) | 59.3 | 9'', 10'' |

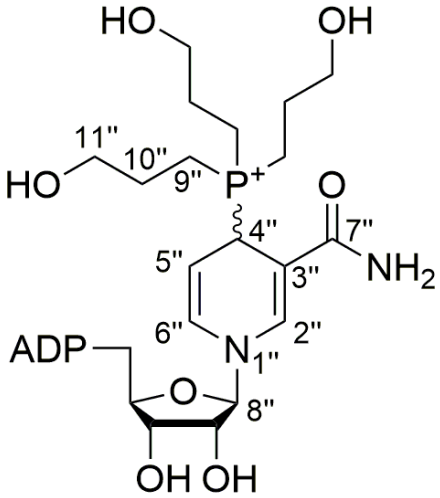


†Chemical shifts were determined from the one dimensional $^{1}H$ and $^{13}C$ experiments. Correlations were determined from $^{1}H$-$^{13}C$ HSQC and HMBC experiments shown in SI Fig. 7 and correspond to site labels shown above in the $NAD^{+}$–THPP reaction product structure.
‡Listed next to each $^{1}H$-NMR or $^{13}C$-NMR chemical shift value is (multiplicity designation [s, singlet; d, doublet; m, multiplet; etc.], integral value, and J-coupling constant).

## SI Table 6. X-ray diffraction data collection and refinement statistics

| Parameter | |
|---|---|
| PDB ID | 5VPS |
| Space group | $P4_22_12$ |
| *Unit-cell parameters* | |
| $a = b$ (Å) | 64.09 |
| $c$ (Å) | 119.17 |
| $\alpha = \beta = \gamma$ | 90º |
| Matthews coefficient (Å$^3$Da$^{-1}$) | 2.22 |
| Solvent content (%) | 44.5 |
| Resolution range (Å) | 50 – 1.45 (1.49 – 1.45)[a] |
| Mean I/$\sigma$(I) | 30.0 (3.44) |
| No. of observed reflections | 44,832 (3280) |
| Completeness (%) | 100 (100) |
| Multiplicity | 10.2 (7.1) |
| $R_{merge}$ | 0.051 (0.574) |
| ***Refinement*** | |
| No. of used reflections | 44,828 |
| $R_{work}$ (%) | 0.149 |
| $R_{free}$ (%) | 0.164 |
| Mean B factor (Å$^2$) | 17.9 |
| RMSD bonds (Å) | 0.006 |
| RMSD angles (°) | 1.146 |

***Model Validation***

| | |
|---|---|
| Clash score, all atoms | 2.77 |
| Ramachandran Favored (%) | 98.1 |
| Ramachandran Outliers (%) | 0 |
| Poor Rotamers (%) | 0 |
| MolProbity score | 1.06 |

[a] Value in parenthesis are statistics for the highest resolution shell.

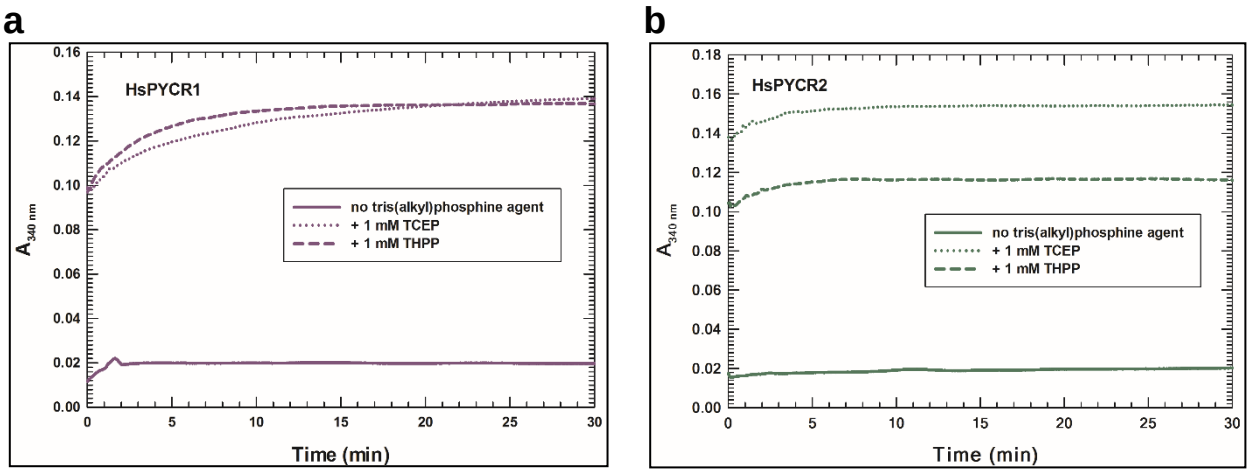


**SI Figure 1. Test for PYCR activity in the reverse direction.** PYCR activity in the reverse direction (L-Pro + $NAD^+$ → L-P5C + NADH) was assayed using 0.06 µM (a) HsPYCR1 or (b) HsPYCR2. Assays were performed in 0.1 M Tris-HCl (pH 7.5) buffer with 0.01% (v/v) Brij-35 detergent, 30 mM $MgCl_2$, 5 mM L-proline, 0.5 mM $NAD^+$, and with or without 1 mM TCEP or 1 mM THPP. The absorbance at 340 nm was recorded for 30 min.

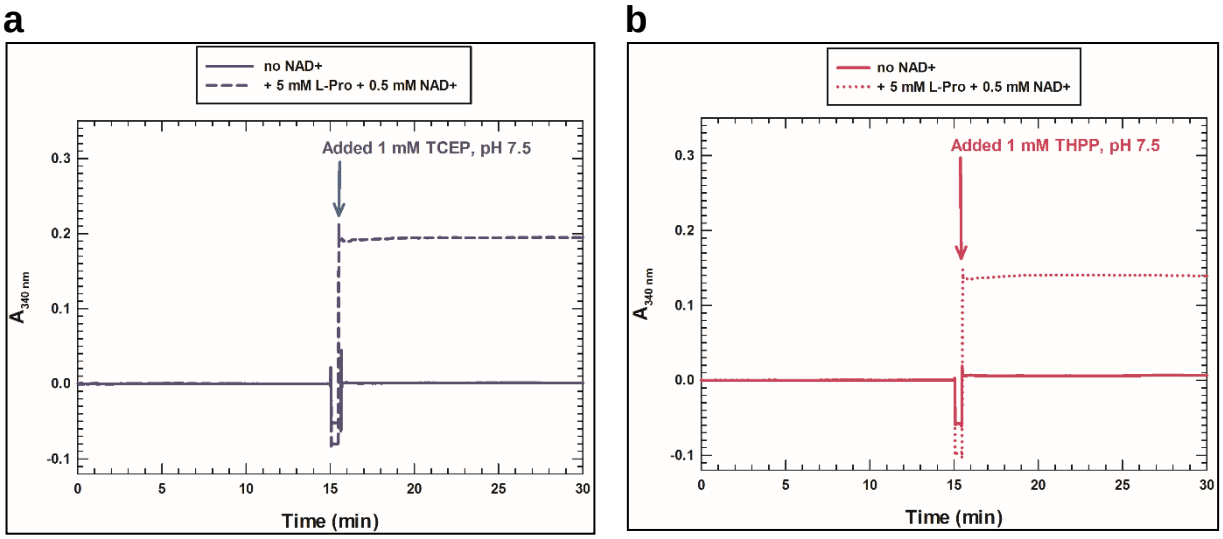


**SI Figure 2. Absorbance changes upon mixing $NAD^+$ with tris(alkyl)phosphine compounds.** $NAD^+$ (0.5 mM) was incubated in 0.1 M Tris-HCl (pH 7.5) buffer with 0.01% (v/v) Brij-35 detergent, 30 mM $MgCl_2$, and 5 mM L-proline. After 15 min, (a) TCEP and (b) THPP were added (1 mM final concentration) and the absorbance was recorded for an additional 15 min.

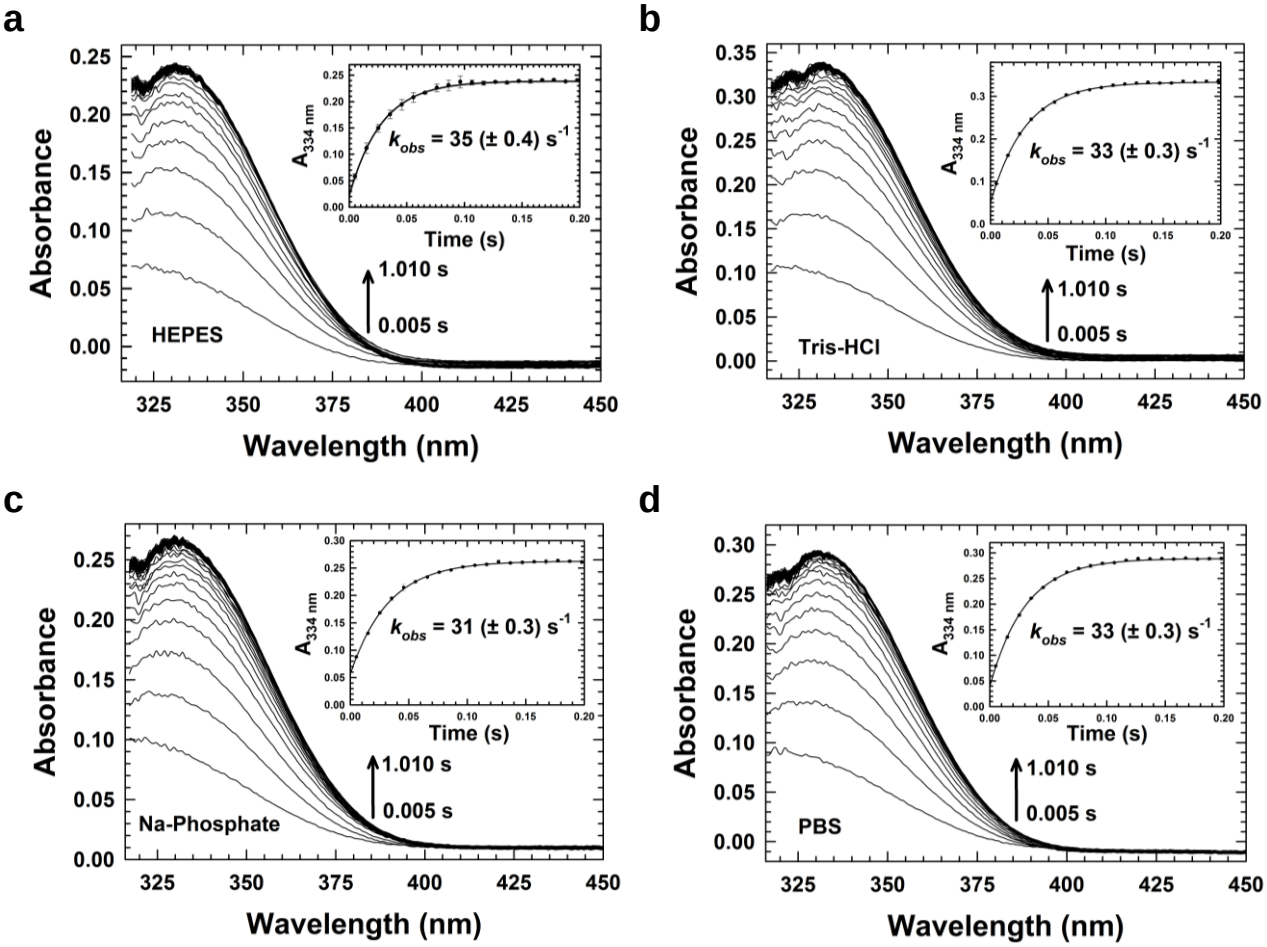


**SI Figure 3. Stopped-flow absorbance spectrophotometry of mixing $NAD^+$ and TCEP.** $NAD^+$ (0.5 mM after mixing) and TCEP (25 mM after mixing) were rapidly combined and multiwavelength absorbance traces were recorded. Reactions were performed in 100 mM (pH 7.5) (a) HEPES, (b) Tris-HCl, (c) Na-Phosphate, and (d) PBS reaction buffer. Plots of the absorbance increase at 334 nm fit to a single 3 parameter exponential equation are shown in the inset along with the observed rate constant ($k_{obs}$).

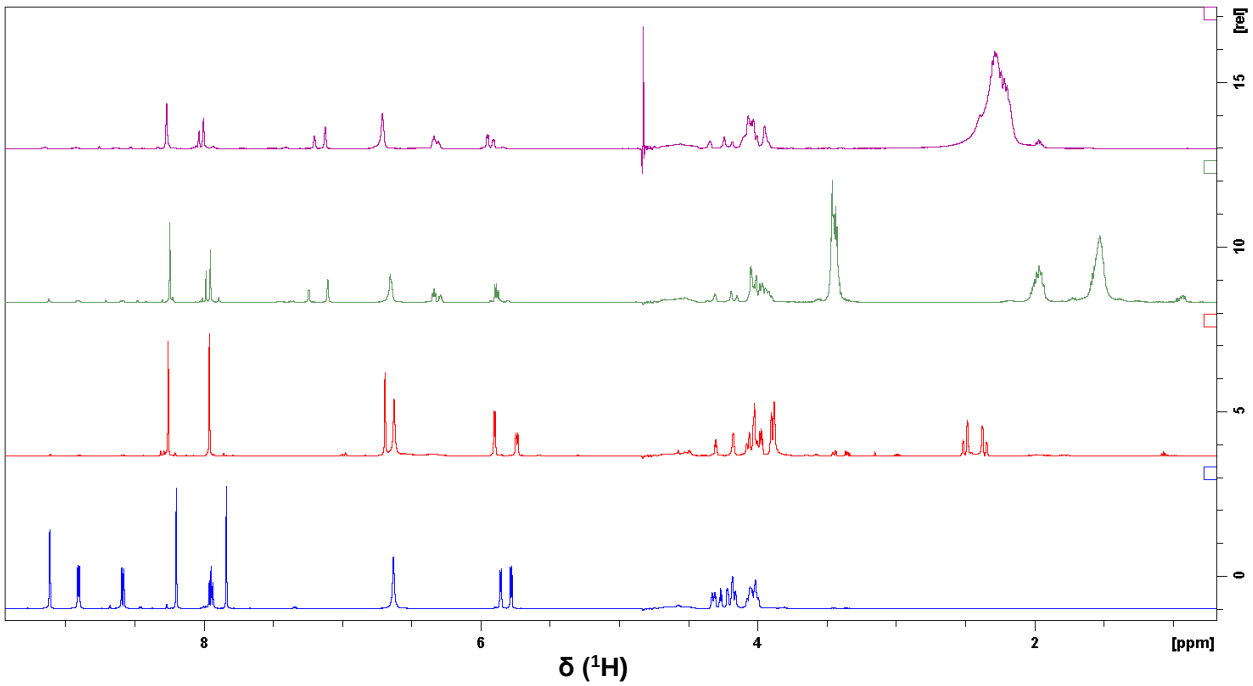


**SI Figure 4.** Stacked proton NMR spectra of $NAD^+$(blue), NADH (red), and reaction mixtures of $NAD^+$ with THPP (green) or TCEP (fuchsia).

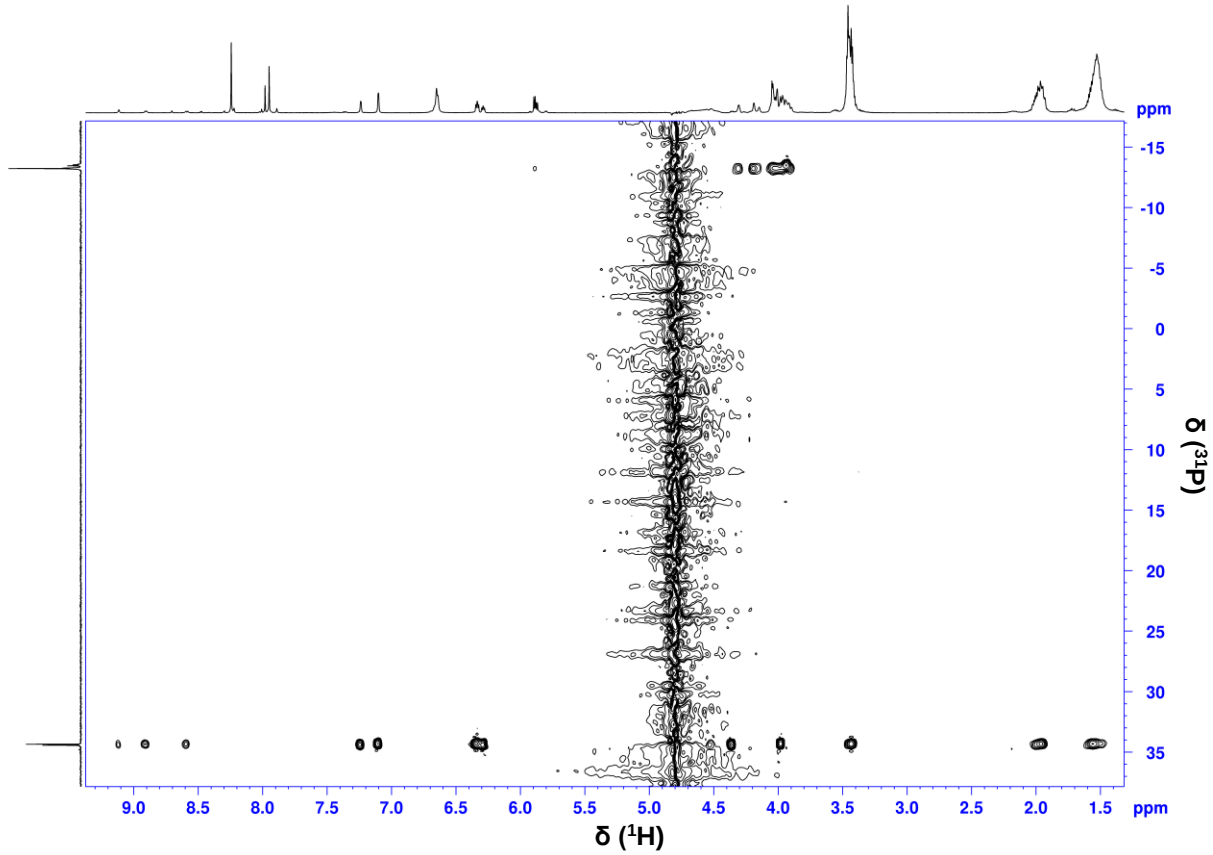


**SI Figure 5.** Two-dimensional $^{1}$H-$^{31}$P HSQC-TOCSY spectra of NAD$^{+}$ and THPP reaction mixture. The spectrum was acquired with a J(HP)-coupling constant of 11 Hz and a TOCSY mixing time of 80 ms. The assignment of this spectra is summarized in SI Table 4. Note the $^{1}$H-$^{31}$P correlations shown here correspond to both NAD$^{+}$–THPP reaction product protons and to NAD$^{+}$ protons.

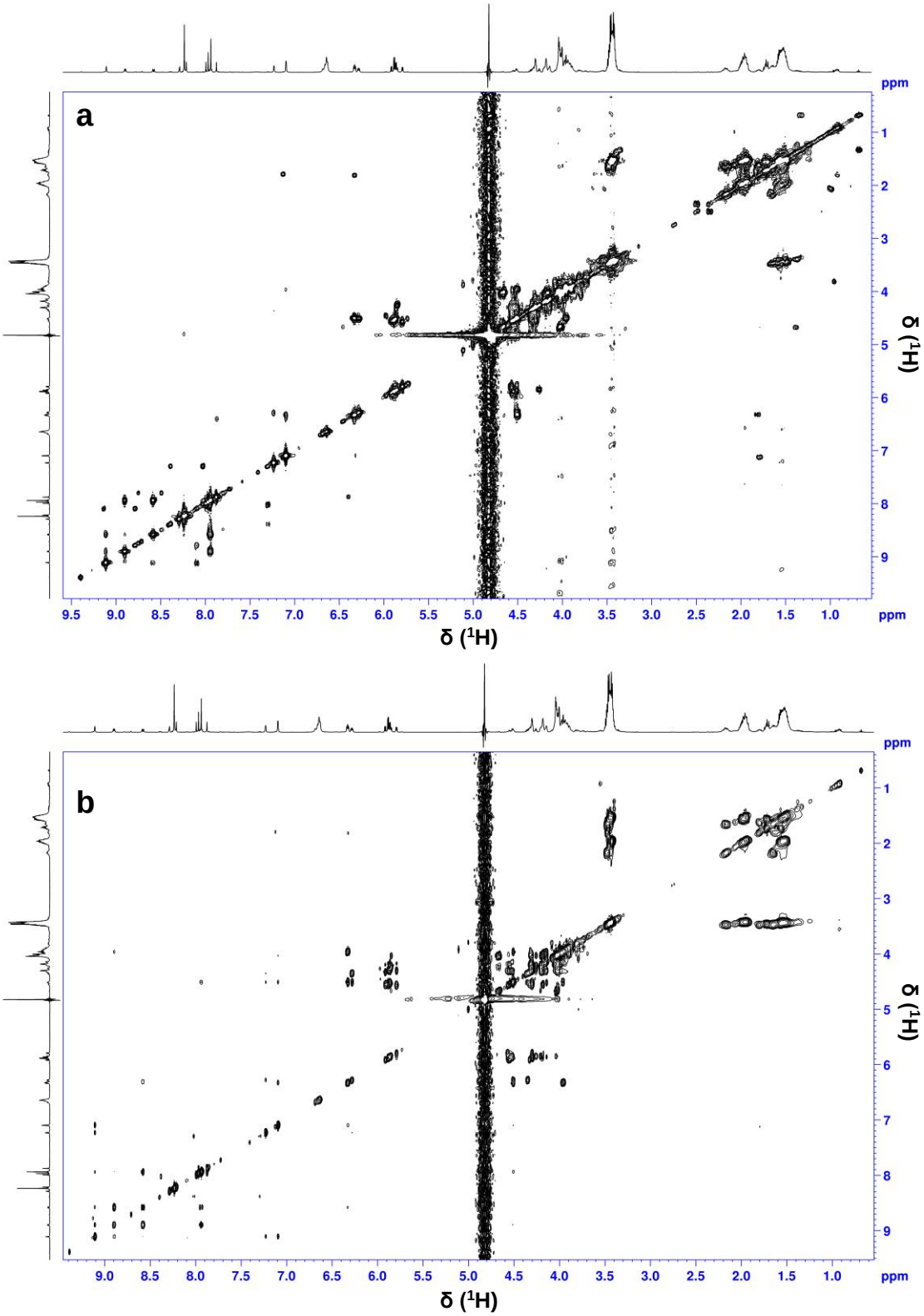


**SI Figure 6.** Two-dimensional (a) $^{1}$H-$^{1}$H COSY spectrum and (b) $^{1}$H-$^{1}$H TOCSY spectrum of $NAD^{+}$ and THPP reaction mixture.

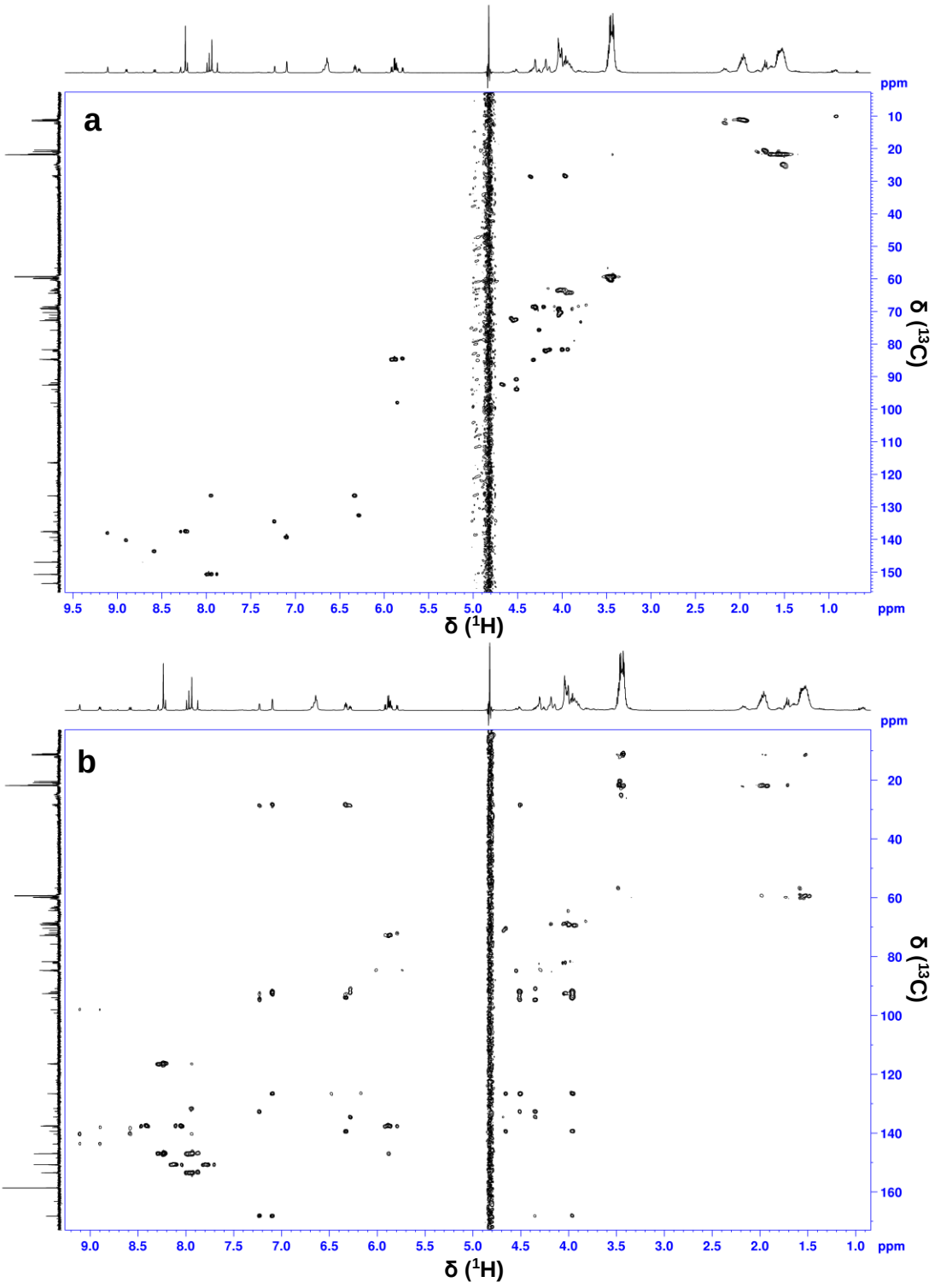


**SI Figure 7.** Two-dimensional (a) $^{1}H$-$^{13}C$ HSQC spectrum and (b) $^{1}H$-$^{13}C$ HMBC spectrum of $NAD^{+}$ and THPP reaction mixture. The assignments of these spectra are summarized in SI Table 5.

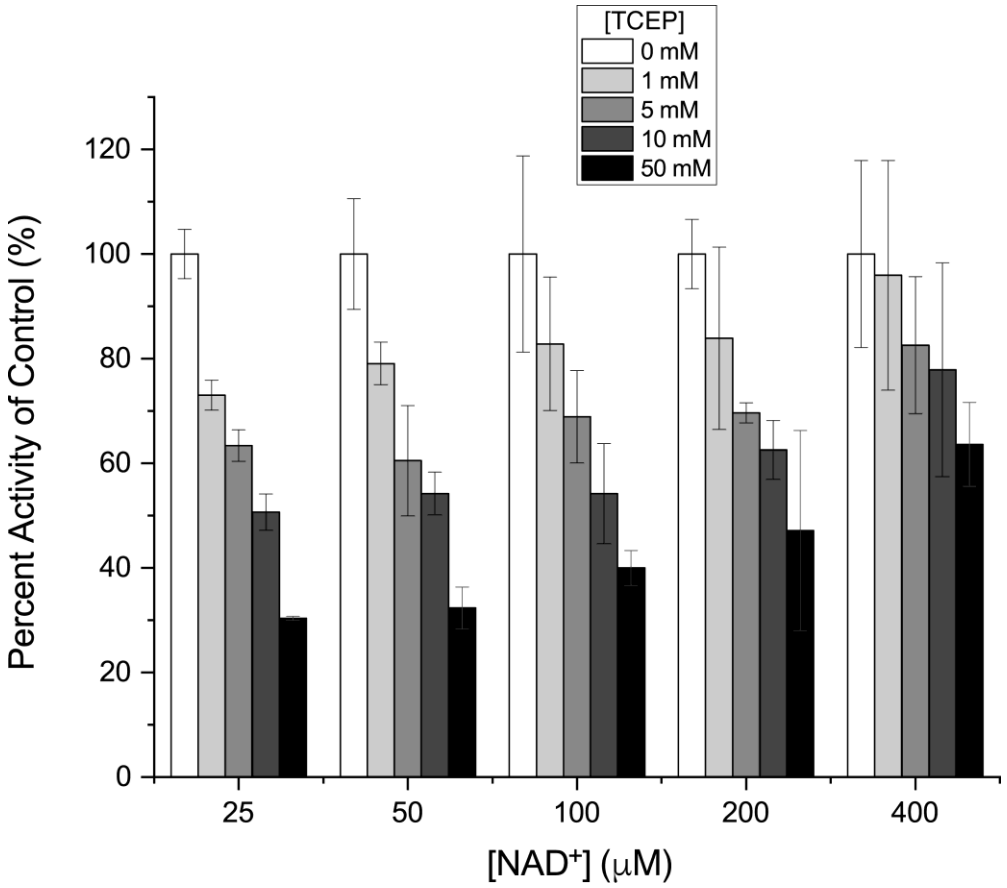


**SI Figure 8.** Interference of an assay of glucose-6-phosphate dehydrogenase by TCEP. The bars represent the apparent reaction rate as a function of $NAD^+$ and TCEP concentrations, with G6P fixed at 5 mM. For each $NAD^+$ concentration, the results are normalized to the rate measured in the absence of TCEP. The error bars represent the absolute difference between two trials.

## REFERENCES


(1) Ruszkowski, M., Nocek, B., Forlani, G., and Dauter, Z. (2015) The structure of *Medicago truncatula* delta(1)-pyrroline-5-carboxylate reductase provides new insights into regulation of proline biosynthesis in plants. *Front. Plant Sci. 6*, 869.

(2) Haid, E., Lehmann, P., and Ziegenhorn, J. (1975) Molar absorptivities of beta-NADH and beta-NAD at 260 nm. *Clin. Chem. 21*, 884-887.

(3) Christensen, E. M., Patel, S. M., Korasick, D. A., Campbell, A. C., Krause, K. L., Becker, D. F., and Tanner, J. J. (2017) Resolving the cofactor-binding site in the proline biosynthetic enzyme human pyrroline-5-carboxylate reductase 1. *J. Biol. Chem. 292*, 7233-7243.

(4) Pollard, T. D., and De La Cruz, E. M. (2013) Take advantage of time in your experiments: a guide to simple, informative kinetics assays. *Mol. Biol. Cell. 24*, 1103-1110.

(5) Bryan, C. M., Bhandari, J., Napuli, A. J., Leibly, D. J., Choi, R., Kelley, A., Van Voorhis, W. C., Edwards, T. E., and Stewart, L. J. (2011) High-throughput protein production and purification at the Seattle Structural Genomics Center for Infectious Disease. *Acta Crystallogr. Sect. F Struct. Biol. Cryst. Commun. 67*, 1010-1014.

(6) Choi, R., Kelley, A., Leibly, D., Hewitt, S. N., Napuli, A., and Van Voorhis, W. (2011) Immobilized metal-affinity chromatography protein-recovery screening is predictive of crystallographic structure success. *Acta Crystallogr. Sect. F Struct. Biol. Cryst. Commun. 67*, 998-1005.

(7) Kabsch, W. (2010) Xds. *Acta Crystallogr. D Biol.Crystallogr. 66*, 125-132.

(8) Vagin, A., and Teplyakov, A. (2010) Molecular replacement with MOLREP. *Acta Crystallogr. D Biol. Crystallogr. 66*, 22-25.

(9) Adams, P. D., Afonine, P. V., Bunkoczi, G., Chen, V. B., Davis, I. W., Echols, N., Headd, J. J., Hung, L. W., Kapral, G. J., Grosse-Kunstleve, R. W., McCoy, A. J., Moriarty, N. W., Oeffner, R., Read, R. J., Richardson, D. C., Richardson, J. S., Terwilliger, T. C., and Zwart, P. H. (2010) PHENIX: a comprehensive Python-based system for macromolecular structure solution. *Acta Crystallogr. D Biol. Crystallogr. 66*, 213-221.

(10) Emsley, P., and Cowtan, K. (2004) Coot: model-building tools for molecular graphics. *Acta Crystallogr. D Biol. Crystallogr. 60*, 2126-2132.

(11) Liu, W., Hancock, C. N., Fischer, J. W., Harman, M., and Phang, J. M. (2015) Proline biosynthesis augments tumor cell growth and aerobic glycolysis: involvement of pyridine nucleotides. *Sci Rep 5*, 17206.